

# Direct observation of vacuum fluctuations in a spinor Bose-Einstein condensate

Carsten Klempt,<sup>1</sup> Oliver Topic,<sup>1</sup> Gebremedhn Gebreyesus,<sup>2</sup> Manuel Scherer,<sup>1</sup> Thorsten Henninger,<sup>1</sup> Philipp Hyllus,<sup>2</sup> Wolfgang Ertmer,<sup>1</sup> Luis Santos,<sup>2</sup> and Jan Arlt<sup>1</sup>

<sup>1</sup>*Institut für Quantenoptik, Leibniz Universität Hannover, Welfengarten 1, D-30167 Hannover, Germany*

<sup>2</sup>*Institut für Theoretische Physik, Leibniz Universität Hannover, Welfengarten 1, D-30167 Hannover, Germany*

(Dated: December 22, 2018)

The nature of the vacuum state and its fluctuations constitutes one of the most fascinating aspects of modern physics. Despite their non-intuitive character, vacuum fluctuations play an important role for our understanding of nature. Specifically, the parametric amplification of such fluctuations is crucial for phenomena ranging from optical parametric down-conversion [1] to stimulated positronium annihilation [2], and boson creation in Universe inflation [3]. Spinor Bose-Einstein condensates [4, 5, 6, 7], consisting of atoms with non-zero total spin, provide an optimal system for the investigation of the vacuum state [8, 9], since vacuum fluctuations can dominate classical fluctuations in the spin dynamics of these magnetic superfluids. Here we explore the amplification of vacuum fluctuations in gaseous spinor condensates in an unstable spin configuration. We observe strong instability resonances in the spinor condensate, induced by the confinement of the atomic ensemble. Our work shows that it is crucial for the understanding of spinor dynamics to consider this confinement, which has previously been neglected in homogeneous approximations [4, 5, 6, 7, 8, 9]. On these resonances we conclusively demonstrate that the system can act as a parametric amplifier for vacuum fluctuations, providing a new microscope to investigate the vacuum state and a promising method for entanglement and squeezing production in matter waves [10, 11].

The behaviour of spinor gases, consisting of atoms with non-zero spin  $F$ , is governed by spin-dependent collisional interactions, the Zeeman energy of the spin states, and the external confinement of the ensemble. Out of equilibrium, spin changing collisions allow for a coherent transfer between spin components [6, 12, 13]. The Zeeman energy suppresses this effect for sufficiently high magnetic fields. However, at low fields the interplay between Zeeman and interaction energy leads to an intriguing spin mixing efficiency which may show a pronounced maximum [14, 15, 16, 17].

The spinor dynamics is best understood by considering the spin excitation modes [8] of the initial Bose-Einstein condensate (BEC). Depending on the magnetic field and the interactions, these modes may become dynamically unstable, initiating the spinor dynamics. This picture allows for a good understanding of recent experiments in  $^{87}\text{Rb}$  ensembles [7, 18, 19, 20] with  $F = 1$ . The case of a BEC initially in a state with a spin projection  $m_F = 0$  is particularly fascinating [9, 12]. In this case, spin-changing collisions lead to the creation of entangled Einstein-Podolsky-Rosen [11, 21] pairs in  $m_F \neq 0$  states, which exponentially grow in number by parametric amplification.

To initiate our experiments, we prepare BECs containing  $7 \times 10^4$   $^{87}\text{Rb}$  atoms in the state with  $F = 2$  and  $m_F = 0$  (denoted by  $|m_F = 0\rangle$ ) in an optical dipole trap with trapping frequencies of (176, 132, 46) Hz. We carefully remove residual atoms in other spin components by briefly applying a strong magnetic field gradient of  $\approx 50$  G/cm. After this purification, the applied homogeneous magnetic field is lowered from 7.9 G to a specific value between 0.12 and 2 G within 3 ms. The BEC is

held at the chosen magnetic field for a variable time to allow for spin changing collisions. Finally, the number of atoms in all  $m_F$  components is measured independently by applying a strong magnetic field gradient during time-of-flight expansion. The whole sequence is illustrated for two specific magnetic fields in Fig. 1.

To evaluate the onset of the exponential amplification regime, we restrict our investigation to short spin evolution times and small populations in the states  $|\pm 1\rangle$ . Figure 2 (a) shows the magnetic field dependence of the fraction of atoms transferred into the  $|\pm 1\rangle$  states after an evolution time of 21 ms. As expected [6], no atoms in the  $|\pm 2\rangle$  states were detected at this time scale. The transferred fraction of atoms in the  $|\pm 1\rangle$  states shows a striking multi-resonant magnetic field dependence, which is directly linked to the interplay between the Zeeman energy and the confinement of the ensemble.

A spinor BEC initially prepared in the  $|0\rangle$  state is represented by a vector field  $\Psi_0(\vec{r}) = (\psi_{-2}, \psi_{-1}, \psi_0, \psi_1, \psi_2)^T = (0, 0, n_0(\vec{r})^{1/2}, 0, 0)^T$ . The onset of the transfer between spin components (linear regime) is described by a spinor operator  $\hat{\Psi}(\vec{r}, t) = (\Psi_0(\vec{r}) + \delta\hat{\Psi}(\vec{r}, t))e^{-i\mu t}$ , where  $\mu$  is the chemical potential,  $\delta\hat{\Psi}(\vec{r}, t) = (\delta\hat{\psi}_{-2}, \delta\hat{\psi}_{-1}, \delta\hat{\psi}_0, \delta\hat{\psi}_1, \delta\hat{\psi}_2)^T$  is the operator for the spin fluctuations, and the density fulfils the condition  $n_0(\vec{r}) \gg \langle \delta\hat{\psi}_{m_F}^\dagger(\vec{r}) \delta\hat{\psi}_{m_F}(\vec{r}) \rangle$ . Up to second order in  $\delta\hat{\psi}_{m_F}$  we obtain a Hamiltonian for the pair creation in the  $|\pm 1\rangle$  states [8]:

$$\hat{H} = \int d^3\vec{r} \left\{ \sum_{m_F=\pm 1} \delta\hat{\psi}_{m_F}^\dagger \left[ \hat{H}_{eff} + q \right] \delta\hat{\psi}_{m_F} + \Omega_{eff}(\vec{r}) \left[ \delta\hat{\psi}_1^\dagger \delta\hat{\psi}_{-1}^\dagger + \delta\hat{\psi}_1 \delta\hat{\psi}_{-1} \right] \right\}, \quad (1)$$

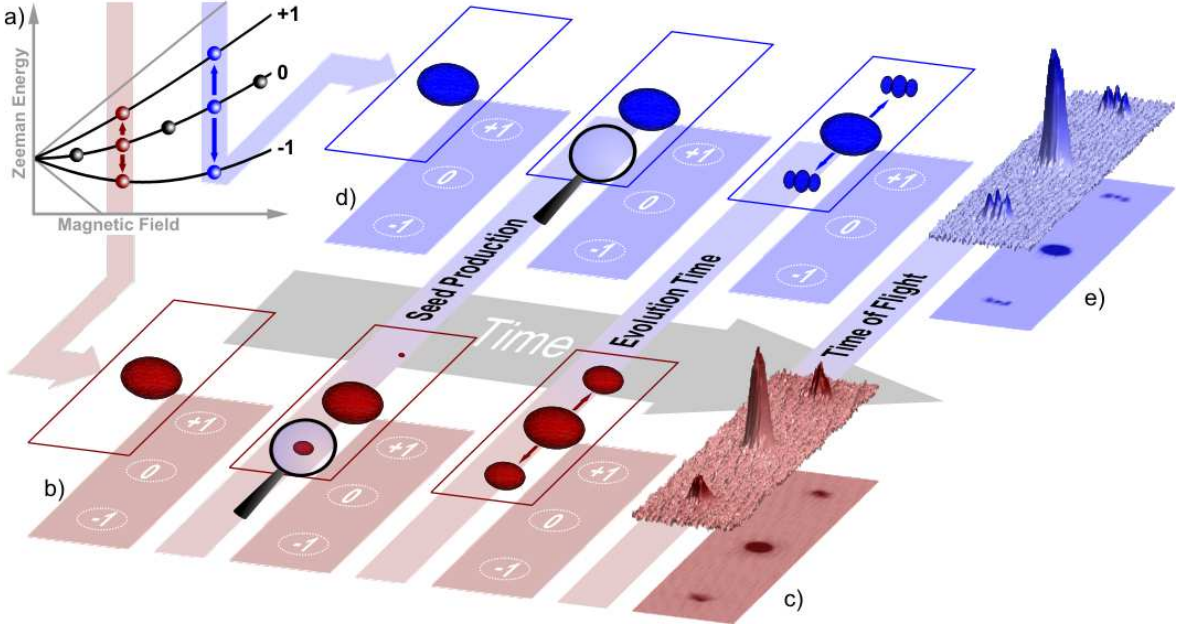


FIG. 1: Observation of resonantly amplified vacuum fluctuations in a spinor condensate. (a) Zeeman energy of the spin states of  $^{87}\text{Rb}$  in the  $F = 2$  state. The two investigated instability resonances are indicated in red and blue. At these resonances atom pairs in the  $|m_F = \pm 1\rangle$  states are produced in specific spatial modes supported by the confining potential. The experimental procedure to investigate this process is shown in rows (b) and (d). (b) At the first resonance (red) a small number of seed atoms in the  $|m_F = \pm 1\rangle$  states (indicated by the magnifying glass) is always produced in the appropriate mode, either deliberately or accidentally. During the evolution time, the unstable condensate amplifies the seed exponentially in that particular spatial mode. Finally the spin states are separated during time-of-flight expansion, and the spatial profiles (c) of the three spin components are recorded in an absorption image. (d) The spatial mode corresponding to the second resonance (blue) is not accessible for classical seed atoms, and therefore remains a pure vacuum state. During the evolution time, the fluctuations of this vacuum state are amplified. (e) The absorption image at the second resonance shows the spatial mode of the amplified vacuum fluctuations, in agreement with numerical simulations of its velocity distribution [22].

where  $q \propto B^2$  describes the quadratic Zeeman energy, and  $B$  is the applied magnetic field. The effective Hamiltonian for the spin components  $|\pm 1\rangle$  is  $\hat{H}_{eff} = -\hbar^2 \nabla^2 / 2m + V(\vec{r}) + 2(U_0 + U_1)n_0(\vec{r}) - \mu$ , where  $m$  is the atomic mass, and  $V(\vec{r})$  is the confining potential. The coupling coefficient  $\Omega_{eff}(\vec{r}) = U_1 n_0(\vec{r})$  characterizes the pair creation induced by spin-changing collisions and the interaction strengths  $U_0$ ,  $U_1$  are determined by the  $s$ -wave scattering lengths for the available collisional channels [4]. Again, we neglect the  $|\pm 2\rangle$  states due to the much lower transfer rate from  $|0\rangle$ . This Hamiltonian  $\hat{H}$  is identical to the one describing optical parametric amplification [8].

For homogeneous BECs,  $V_{eff}$  and  $\Omega_{eff}$  are constants, and the spin excitations are plane waves with wavevector  $\vec{k}$  and energy  $\xi_k(q)$  obtained from Eq. (1). If the imaginary part of the energy  $\text{Im}(\xi_k(q))$  is positive for some  $k$ , the BEC in  $|0\rangle$  is dynamically unstable and pair production into the  $|\pm 1\rangle$  state occurs. By adapting the result of ref. [8] to the case of  $^{87}\text{Rb}$  in the  $F = 2$  state (where  $U_1 > 0$  and  $q < 0$ ) one obtains three regimes, which can be classified according to the quadratic Zeeman effect. BECs in the  $|0\rangle$  state are (i) stable for  $q > 0$ ; (ii) unstable for  $q_{cr} \equiv -n_0 U_1 < q < 0$ , where

the instability rate of the most unstable mode (with  $k_{\max} = 0$ ) is  $\Lambda(q) = \sqrt{q_{cr}^2 - (q - q_{cr})^2} / \hbar$ ; (iii) unstable for  $q < q_{cr}$  with a constant instability rate  $\Lambda(q) = |q_{cr}| / \hbar$  for the most unstable modes  $\hbar^2 k_{\max}^2 / 2m = q_{cr} - q$  (see Fig. 3). This dependence of the instability rate  $\Lambda(q)$  on the quadratic Zeeman effect directly yields the magnetic field dependence of the pair creation efficiency.

Although this simplified homogeneous picture offers important insights, the observed magnetic field dependence of the spinor dynamics in confined BECs is crucially different, showing that the confinement must be included to obtain even a qualitative understanding of our experimental results. In the confined case, the excitations  $\xi_\nu(q)$  are again obtained by diagonalizing  $\hat{H}$ . Figure 3 shows the magnetic field dependence of the maximal instability rate  $\Lambda(q) = \max_\nu |\text{Im}(\xi_\nu(q))| / \hbar$  for the experimental parameters of Fig. 2 (a). In the unstable regime with low  $|q|$  we may approximate the maximal instability rate by  $\Lambda(q) \simeq \sqrt{q_{cr}^2 - (q - \tilde{q}_{cr})^2} / \hbar$  with an effective  $\tilde{q}_{cr}$ . However, this growth is not followed by a constant instability rate for larger  $|q|$ . On the contrary,  $\Lambda(q)$  shows pronounced maxima and minima, which result in a strongly enhanced or inhibited transfer to the  $|\pm 1\rangle$  states in agreement with Fig. 2 (a). This depen-

dence may be also observed in experiments with BECs of other atomic species or spin states. For the case of  $^{87}\text{Rb}$  in  $F = 1$  in ref. [9] we predict a single resonance with a maximal conversion efficiency at  $q = 0$ , and a complete suppression of the pair creation for  $q/h \leq -7$  Hz, in excellent agreement with the reported results.

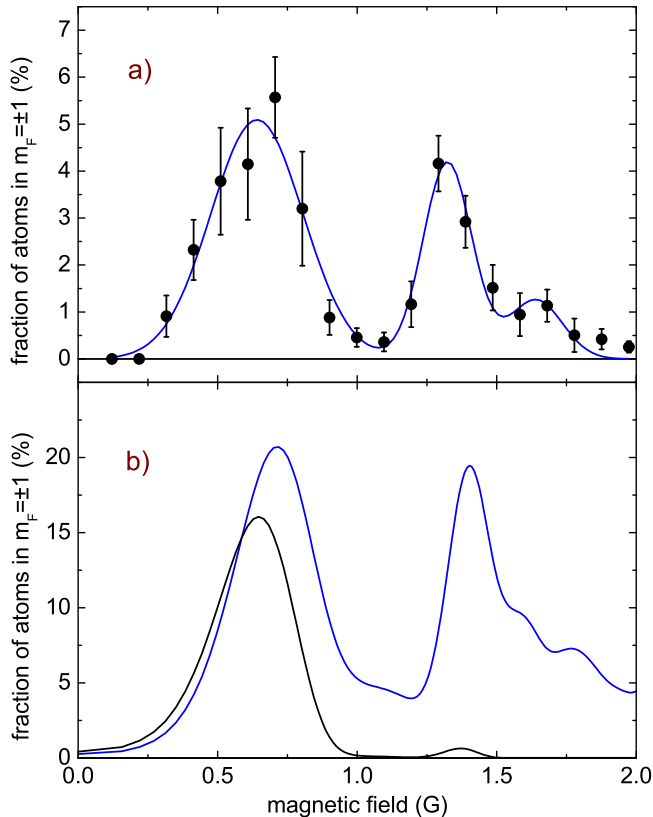


FIG. 2: Multi-resonant spin evolution in a confined Bose-Einstein condensate. (a) Fraction of atoms transferred to the  $|m_F = \pm 1\rangle$  states within 21 ms as a function of the applied magnetic field. To obtain this fraction, the number of transferred atoms per state was divided by the sum of transferred  $|m_F = \pm 1\rangle$  and condensed  $|m_F = 0\rangle$  atoms. Due to strong shot-to-shot fluctuations 15 independent realizations were averaged at each magnetic field. The error bars indicate statistical uncertainties. The blue line is a triple Gaussian fit to guide the eye. (b) Theoretical prediction for the same parameters. The black line shows the results of a mean field calculation with a classical seed of 3.5 atoms, and the blue line shows the results of our Heisenberg simulation including both this classical seed and the vacuum spin fluctuations.

As shown above, pair creation is dominated by the most unstable spin excitation mode at each magnetic field. For a BEC prepared purely in the  $|0\rangle$  state this spinor dynamics is initiated by vacuum spin fluctuations in the  $|\pm 1\rangle$  state. However, this process must be investigated particularly carefully, since even very small populations in  $|\pm 1\rangle$ , created during the preparation stage, may play an important role. The vacuum fluctuations as well as such classical seed contributions in the most un-

stable spin excitation mode are exponentially amplified, since pair creation acts as a parametric amplifier [8, 9].

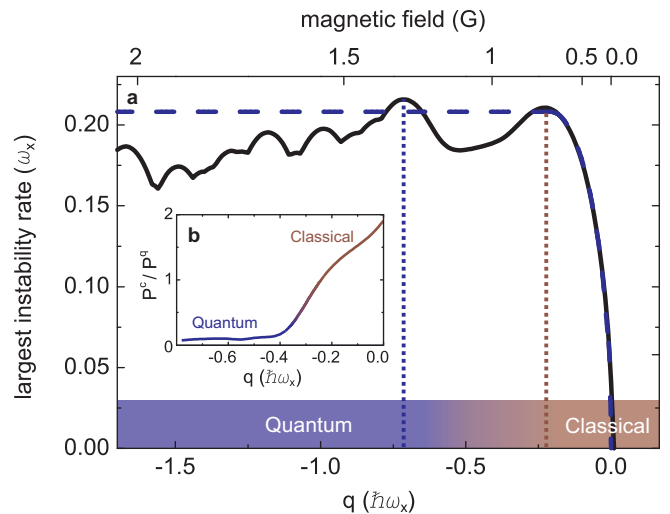


FIG. 3: Maximal instability rate of a confined spinor Bose-Einstein condensate. The instability rate of the most unstable mode (in units of the largest trapping frequency  $\omega_x = 2\pi \times 176$  Hz), corresponding to the pair creation efficiency in the  $|m_F = \pm 1\rangle$  states, is shown as a function of the quadratic Zeeman energy, obtained from a Heisenberg description (solid line). The maximal instability rate for an effective homogeneous case (dotted line) indicates the absence of resonant features in this situation. Inset: Ratio between the classically-triggered  $P^c$  and quantum-triggered  $P^q$  populations, considering only the growth due to the most unstable mode. The quantum triggered dynamics is characterized by  $P^c \ll P^q$ .

In the following we show that we can experimentally distinguish between the amplification of a classical seed and of pure vacuum fluctuations. We observe large fluctuations in the number of atoms transferred into the  $|\pm 1\rangle$  state, which may be traced back to four main effects: (i) The detection of a few thousand atoms has a significant statistical uncertainty. (ii) Small shot-to-shot deviations of the total atom number result in density fluctuations, which lead to strong fluctuations in the pair creation efficiency due to its exponential density dependence. (iii) The number of accidentally generated seed atoms in the  $|\pm 1\rangle$  state may vary from shot-to-shot. (iv) Finally, an amplified pure vacuum state also leads to strong fluctuations in the number of transferred atoms. Due to these effects, a measurement of the magnitude of the fluctuations is not appropriate to identify the triggering mechanism of the observed spin dynamics.

Therefore we investigate the sensitivity of the spinor dynamics to classical seed atoms at the available unstable spin excitation modes. Directly after the purification we deliberately prepare a small number of seed atoms by applying a  $5 \mu\text{s}$  radio frequency (rf) pulse which couples the  $|0\rangle$  state symmetrically to the  $|\pm 1\rangle$  states. For small rf power, it is thus possible to reproducibly prepare a

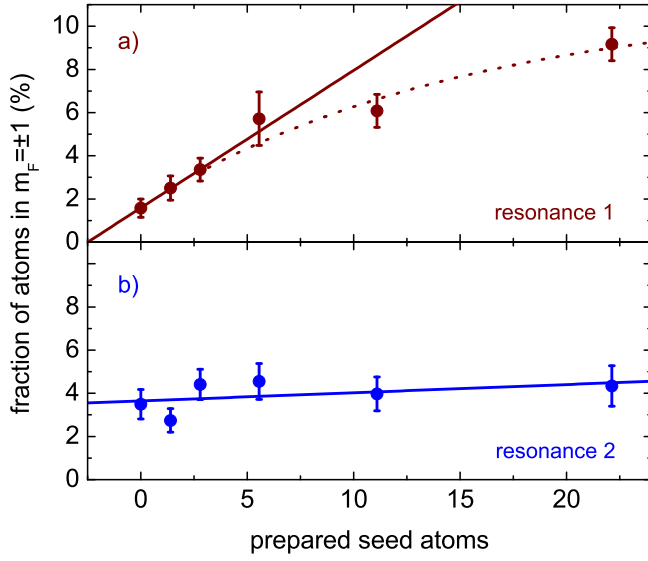


FIG. 4: Amplification of classical and vacuum spin fluctuations. Fraction of atoms transferred to the  $|m_F = \pm 1\rangle$  states as a function of the deliberately prepared number of seed atoms. (a) The fraction recorded at 0.648 G, corresponding to the first resonance, shows a strong dependence on the classical seed after an evolution time of 15 ms. (b), The fraction recorded after 23 ms evolution time on the second resonance at 1.291 G is independent of the number of seed atoms and we conclude that it is triggered by vacuum spin fluctuations. The error bars indicate statistical uncertainties. The solid lines are fits and the dotted line is a guide to the eye indicating saturation.

very small number of seed atoms. Figure 4 (a) shows the dependence of the fraction of transferred atoms on this seed for a magnetic field of 0.648 G, corresponding to the first resonance in Fig. 2(a). Starting at a small offset value, this fraction grows linearly with increasing number of seed atoms (amplification of 23 dB) and starts to saturate for transferred fractions above 6%. The first resonance is hence strikingly sensitive to this classical seed, down to an extremely small seed atom number.

This sensitivity can be investigated theoretically by evaluating the ratio between the classically-triggered ( $P_{\pm 1}^c(t)$ ) and quantum-triggered ( $P_{\pm 1}^q(t)$ ) populations in the  $|\pm 1\rangle$  states for a single initial seed atom, considering only the growth due to the most unstable spin mode  $P_{\pm 1}^c(t) \approx P^c \exp(2\Lambda(q)t)$  and  $P_{\pm 1}^q(t) \approx P^q \exp(2\Lambda(q)t)$ . The ratio  $P^c/P^q$ , shown in Fig. 3 (b), characterizes the quantum or classical nature of the triggering mechanism. For sufficiently low  $|q|$  (including the first resonance), the classical seed is highly relevant due to the large overlap between the wavefunctions of the most unstable mode and the original BEC. In our experiments all seed atoms are produced with this wavefunction, which thus explains the remarkable observed sensitivity. The offset is caused by a small number of classical seed atoms, created by spurious rf and magnetic fields during the 19 ms period

after the purification, as well as by vacuum fluctuations.

However this sensitivity to classical fluctuations is not general. Figure 4 (b) shows the fraction of transferred atoms at a magnetic field of 1.291 G, corresponding to the second resonance in Fig. 2(a). For this field the fraction of transferred atoms is independent of the seed. This shows, that neither deliberately nor accidentally produced seed atoms can trigger the spin dynamics and we hence conclude that the dynamics is solely triggered by vacuum spin fluctuations. This is confirmed by Fig. 3 (b) which shows that the classical seed is irrelevant for sufficiently large  $|q|$  since the overlap of the initial BEC wavefunction and the most unstable spin mode becomes negligible. Similarly, the contribution of the initial thermal cloud in the  $|0\rangle$  state is negligible at any magnetic field due to the lack of significant overlap with the most unstable spin excitations. An equivalent analysis shows that recent amplification experiments [9] could be dominantly quantum-triggered only for  $q/h \lesssim 6$  Hz.

To simulate the linear spinor dynamics, we derive the corresponding Heisenberg equations for  $\delta\hat{\psi}_{\pm 1}$  from Eq. (1). In addition we have taken hyperfine-changing losses [6] into account by introducing an experimentally measured loss rate of  $\Gamma \simeq 10 \text{ s}^{-1}$  for all  $|m_F\rangle$  states. This loss rate was incorporated in the definition of  $\hat{H}_{eff}$  and  $\Omega_{eff}$ . Although these losses are small ( $< 20\%$ ) during a typical experimental sequence, they significantly alter the spinor dynamics due to the dynamical modification of the resonance conditions. Figure 2 (b) shows the numerical result, which is in good agreement with our experimental findings. The unknown average accidental seed, which influences only the first resonance, is obtained from the ratio between the fractions on the two resonances in our experiments. Differences in the absolute value of the transferred fraction can be traced to nonlinear effects as well as experimental uncertainties in the total number of atoms.

Since the second resonance is triggered by vacuum fluctuations, we expect the actual quantum dynamics to differ significantly from the result of a simple mean-field Gross-Pitaevskii (GP) approach in which field operators  $\hat{\psi}_{m_F}(\vec{r})$  are substituted by c-number fields  $\psi_{m_F}(\vec{r})$ . Quantum fluctuations are absent in this description and the spinor dynamics can only be triggered by an initial seed  $\psi_{\pm 1}(\vec{r}) = \epsilon\psi_0(\vec{r})$ , with  $\epsilon \ll 1$  (for more sophisticated approaches, see e.g. ref. [23]). The GP result, using the same parameters as the Heisenberg simulation, is also shown in Fig. 2 (b). The striking difference between GP and Heisenberg results for the same evolution time supports the experimental result, that the spinor dynamics on the second resonance is triggered by vacuum fluctuations. In the GP approach, the second resonance is only recovered after a much longer evolution time due to the extremely small mode overlap.

The amplification of vacuum fluctuations in spinor gases constitutes a promising method for the creation

of entangled atomic Einstein-Podolsky-Rosen-pairs and the squeezing of matter waves [10, 11]. In addition the dipolar interaction may play a significant role [18, 24] in  $F = 1$  condensates and other trapping geometries.

We acknowledge support from the Centre for Quantum Engineering and Space-Time Research QUEST, from the Deutsche Forschungsgemeinschaft (SFB 407), and the European Science Foundation (EuroQUASAR).

- 
- [1] D. F. Walls and G. Milburn, *Quantum Optics* (Springer, ADDRESS, 1994).
  - [2] A. P. Mills, Nucl. Instrum. Methods Phys. Res., Sect. B **192**, 107 (2002).
  - [3] L. Kofman, A. Linde, and A. A. Starobinsky, Phys. Rev. Lett. **73**, 3195 (1994).
  - [4] T.-L. Ho, Phys. Rev. Lett. **81**, 742 (1998).
  - [5] J. Stenger *et al.*, Nature **396**, 345 (1998).
  - [6] H. Schmaljohann *et al.*, Phys. Rev. Lett. **92**, 040402 (2004).
  - [7] L. E. Sadler *et al.*, Nature **443**, 312 (2006).
  - [8] A. Lamacraft, Phys. Rev. Lett. **98**, 160404 (2007).
  - [9] S. R. Leslie *et al.*, arXiv:0806.1553 (2008).
  - [10] L.-M. Duan, A. Sørensen, J. I. Cirac, and P. Zoller, Phys. Rev. Lett. **85**, 3991 (2000).
  - [11] H. Pu and P. Meystre, Phys. Rev. Lett. **85**, 3987 (2000).
  - [12] T. Kuwamoto, K. Araki, T. Eno, and T. Hirano, Phys. Rev. A **69**, 063604 (2004).
  - [13] M.-S. Chang *et al.*, Nature Phys. **1**, 111 (2005).
  - [14] J. Kronjäger *et al.*, Phys. Rev. A **72**, 063619 (2005).
  - [15] W. Zhang *et al.*, Phys. Rev. Lett. **95**, 180403 (2005).
  - [16] J. Kronjäger *et al.*, Phys. Rev. Lett. **97**, 110404 (2006).
  - [17] A. T. Black *et al.*, Phys. Rev. Lett. **99**, 070403 (2007).
  - [18] M. Vengalattore, S. R. Leslie, J. Guzman, and D. M. Stamper-Kurn, Phys. Rev. Lett. **100**, 170403 (2008).
  - [19] R. W. Cherng, V. Gritsev, D. M. Stamper-Kurn, and E. Demler, Phys. Rev. Lett. **100**, 180404 (2008).
  - [20] R. W. Cherng and E. Demler, arXiv:0806.1991v1 (2008).
  - [21] A. Einstein, B. Podolsky, and N. Rosen, Phys. Rev. **47**, 777 (1935).
  - [22] C. Klempt *et al.*, (in preparation).
  - [23] H. Saito, Y. Kawaguchi, and M. Ueda, Phys. Rev. A **76**, 043613 (2007).
  - [24] T. Świsłocki, M. Brewczyk, M. Gajda, and K. Rzkażewski, arXiv:0901.1763 (2009).